NONPOLAR NITRIDE SEMICONDUCTOR OPTOELECTRONIC DEVICES: A DISRUPTIVE TECHNOLOGY FOR NEXT GENERATION ARMY APPLICATIONS

M. Wraback, G.A. Garrett, G.D. Metcalfe, H. Shen
U.S. Army Research Laboratory, Sensors and Electron Devices Directorate, AMSRD-ARL-SE-EM
2800 Powder Mill Road, Adelphi, MD 20783

M. C. Schmidt, A. Hirai, J.S. Speck, S.P. DenBaars, S. Nakamura
Electrical and Computer Engineering and Materials Departments
University of California, Santa Barbara, California 93106

ABSTRACT

Nonpolar nitride semiconductor materials containing a wide range of structural defects are studied. High quality InGaN quantum wells grown on bulk stacking fault (SF) -free GaN substrates show larger PL intensity and shorter PL lifetime with decreasing well width, indicating that the radiative lifetime is becoming smaller as the well narrows, consistent with the theoretically predicted increase in oscillator strength and associated exciton binding energy. Moreover, the fact that these phenomena are observable at room temperature is indicative of the suppression of defect-related nonradiative recombination for growth on bulk substrates, showing great promise for visible light emitters. We have also demonstrated enhanced THz emission from nonpolar GaN due to carrier transport in internal in-plane electric fields created by the termination of the in-plane polarization in wurtzite domains at zincblende stacking faults. The estimated, maximum average in-plane electric field of ~ 290 kV/cm in the wurtzite regions for an I_1 type SF density of 1 X 10^6 cm^{-1} is comparable to the bias fields applied to PC switches using low-temperature grown GaAs, one of the best PC materials, but does not require electrode processing or an external bias. Comparison with THz emission from SF-free m-GaN indicates that the THz signal from SF-related in-plane carrier transport dominates that usually observed from carrier diffusion or surface surge-currents normal to the sample surface, even for high excess electron energies and short absorption lengths favorable to diffusive transport. These results suggest that nonpolar nitride semiconductor devices are a potentially disruptive technology that may lead to leap-ahead advances in devices operating across the electromagnetic spectrum from UV to THz for future Army applications.

1. INTRODUCTION

Group III-V nitride semiconductors, which can be used to fabricate optoelectronic devices spanning the electromagnetic (EM) spectrum from the deep ultraviolet (UV) to terahertz (THz), are important materials for many Army applications, including UV sources and detectors for biodetection, non-line-of-sight covert communications, and water purification, high efficiency visible sources and detectors for energy efficient solid state lighting and full spectrum solar cells, green and frequency doubled green (i.e., deep UV) lasers for water monitoring and bio-identification, and high efficiency THz sources pumped by femtosecond fiber lasers. These compact semiconductor devices can address logistical difficulties associated with the size, weight, cost, ruggedness, and reliability of components that have hindered system deployment. These devices will therefore contribute to the sustainability of the objective force by helping in the reduction of the logistics footprint, while providing new solutions for protection, information, and potable water at the individual soldier level, aiding the survivability, lethality, and deployability of the current and future force.

The growth of nitride semiconductor structures for optoelectronic devices has focused mainly on c-axis oriented wurtzite material where the polar orientation is perpendicular to the growth plane. For light emitting devices such as LEDs and lasers containing multi-

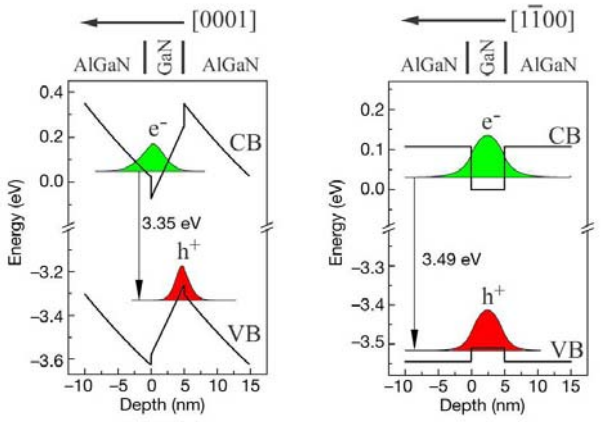

Fig. 1. Comparison of band structure, electron and hole wave functions, and optical transitions in GaN/AlGaN single quantum wells grown along polar (left) and nonpolar directions.

Report Documentation Page

Form Approved
OMB No. 0704-0188

1. REPORT DATE	2. REPORT TYPE	3. DATES COVERED
DEC 2008	**N/A**	**-**

4. TITLE AND SUBTITLE	5a. CONTRACT NUMBER
Nonpolar Nitride Semiconductor Optoelectronic Devices: A Disruptive Technology For Next Generation Army Applications	5b. GRANT NUMBER
	5c. PROGRAM ELEMENT NUMBER
6. AUTHOR(S)	5d. PROJECT NUMBER
	5e. TASK NUMBER
	5f. WORK UNIT NUMBER
7. PERFORMING ORGANIZATION NAME(S) AND ADDRESS(ES) **U.S. Army Research Laboratory, Sensors and Electron Devices Directorate, AMSRD-ARL-SE-EM 2800 Powder Mill Road, Adelphi, MD 20783**	8. PERFORMING ORGANIZATION REPORT NUMBER
9. SPONSORING/MONITORING AGENCY NAME(S) AND ADDRESS(ES)	10. SPONSOR/MONITOR'S ACRONYM(S)
	11. SPONSOR/MONITOR'S REPORT NUMBER(S)

12. DISTRIBUTION/AVAILABILITY STATEMENT
Approved for public release, distribution unlimited

13. SUPPLEMENTARY NOTES
See also ADM002187. Proceedings of the Army Science Conference (26th) Held in Orlando, Florida on 1-4 December 2008, The original document contains color images.

14. ABSTRACT

15. SUBJECT TERMS

16. SECURITY CLASSIFICATION OF:			17. LIMITATION OF ABSTRACT	18. NUMBER OF PAGES	19a. NAME OF RESPONSIBLE PERSON
a. REPORT	b. ABSTRACT	c. THIS PAGE			
unclassified	**unclassified**	**unclassified**	**UU**	**6**	

quantum well (MQW) active regions, electric fields resulting from the termination of the spontaneous and piezoelectric polarizations at the heterointerfaces lead to red-shifts in the emission wavelength due to the quantum confined stark effect (QCSE), and to reduced emission efficiency from the separation of the electron and hole wave functions in the quantum well (Fig. 1). With the advent of bulk nonpolar and semipolar stacking fault (SF)-free GaN substrates, the deleterious effects of these polarization fields can be mitigated in conjunction with defect reduction associated with homoepitaxial growth on a native substrate, potentially enabling the development of UV and visible lasers and LEDs that may achieve optimal performance for the first time (Iso et al., 2007).

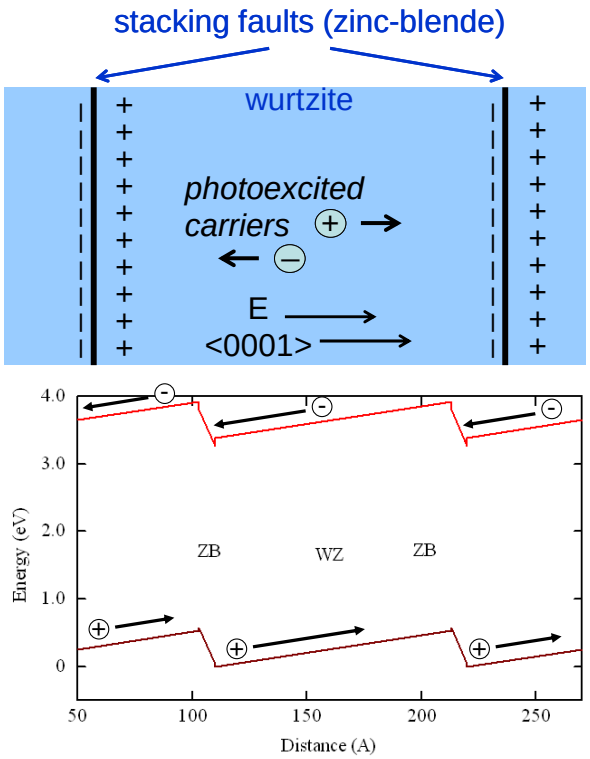

Fig. 2. Schematic showing conceptual drawing of stacking fault terminated polarization and the envisioned effective "lateral bandstructure".

Nevertheless, the spontaneous polarization along the c-axis in nonpolar nitride semiconductors still exists, and a substantial polarization charge can exist at the interfaces of wurtzite domains terminated by zincblende stacking faults in imperfect crystals, leading to large in-plane electric fields (Fig. 2). Since the bandgap of zincblende nitride semiconductors is less than that of comparable wurtzite materials, a lateral "bandstructure" can be envisioned that can be employed in the creation of enhanced THz emission associated with photoexcited in-plane carrier transport on a sub-picosecond time scale.

In this paper, we present fundamental studies of these novel materials and investigate their performance in sources across the EM spectrum. Optical properties of high quality materials for visible laser and LED applications, without appreciable stacking faults or other structural defects, are presented first to illustrate the tremendous promise of these nitride semiconductor materials. These results are followed by studies of nonpolar nitride semiconductors with large stacking fault densities, which we show can be beneficial as high performance sources of THz radiation.

2. OPTICAL PROPERTIES OF HIGH QUALITY NONPOLAR INGAN QUANTUM WELLS

The large oscillator strength and exciton binding energy in GaN quantum wells affords the possibility of high efficiency light emitting devices with shorter radiative lifetimes than those in other III–V semiconductors. This potential is never fully realized in conventional *c*-plane heterostructures because of the large polarization fields in nitride QWs (Bernardini et al., 1997, Im et al., 1998), which increase the radiative lifetime by inhibiting electron–hole wavefunction overlap in the wells (Grandjean et al., 1999, Jho et al., 2002), and because of the high defect density, which leads to short nonradiative lifetimes (Wraback et al., 2007). While growth in nonpolar directions eliminates these polarization fields, providing a means for improved device performance (Waltereit et al., 2000), epilayers on heteroepitaxial structures still have a large density of basal plane stacking faults and threading dislocations. These defects can be significantly reduced in GaN/AlGaN structures using lateral epitaxial overgrowth (LEO) (Haskell et al., 2003), and can be virtually eliminated in InGaN/GaN structures and devices using stacking fault-free bulk GaN substrates (Iso et al., 2007, and references therein). In this study, we use time-resolved photoluminescence (TRPL) to probe the relation between radiative lifetime and well width in high quality m-plane InGaN/GaN single quantum wells on bulk stacking fault-free GaN substrates.

Figure 3 shows time-resolved photoluminescence (TRPL) and PL spectra from single InGaN/GaN QWs with well widths varying from 2 nm to 16 nm. The samples were excited using ~ 100-fs pulses at 378 nm from a frequency doubled optical parametric amplifier pumped by an amplified Ti:Sapphire pulsed laser, enabling direct excitation of the InGaN QWs below the GaN barriers. As a function of increasing well width, the measured PL lifetime is found to increase from 1.25 ns for a 2 nm well to 5.9 ns for a 16 nm well. While variations in In content for the various well widths cause some scatter in the data, concurrent measurements of the time-integrated PL spectra show an increase in the PL

intensity (scaled to emitting volume) for thinner wells, along with a blue shift in energy from quantum confinement. The observation of larger PL intensity and shorter PL lifetime with decreasing well width suggests that the radiative lifetime is becoming smaller as the well narrows, consistent with the theoretically predicted increase in oscillator strength and associated exciton binding energy, as well as previous measurements of GaN/AlGaN MQWs on LEO GaN templates (Garrett et al., 2005).

Temperature dependent measurements of this phenomenon provide further verification of our hypothesis. Figure 4 shows the temperature dependence of the PL lifetime and the radiative lifetime calculated from this quantity and temperature dependent time-integrated PL for the 2 nm, 6 nm, and 16 nm QWs. For all three samples the PL lifetime decreases monotonically with decreasing temperature, becoming nearly

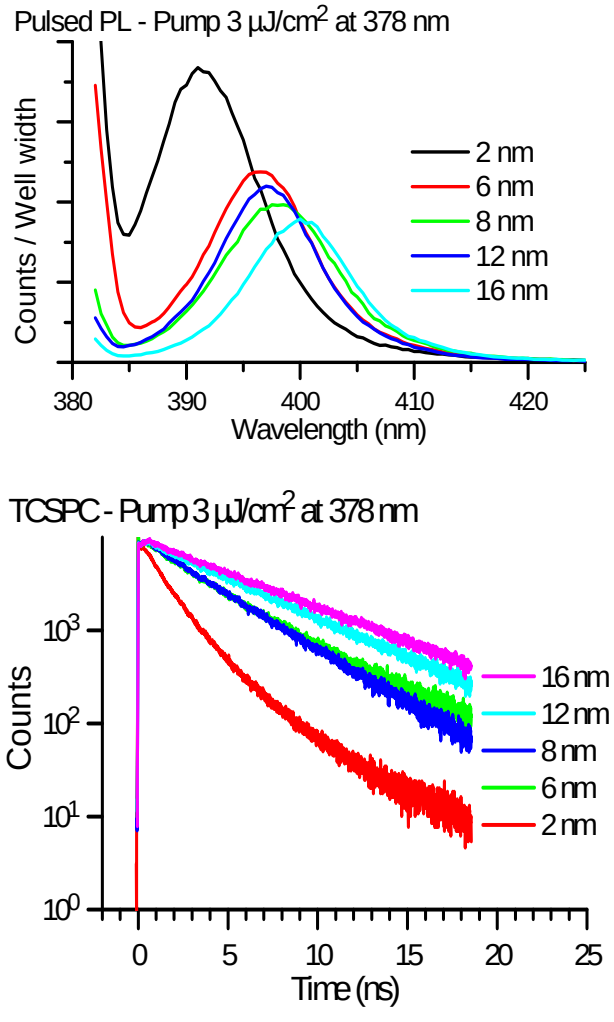

Fig. 3. Time-integrated PL spectra (top) and TRPL (bottom) for a series of InGaN/GaN SQWs on *m*-plane bulk SF-free GaN substrates.

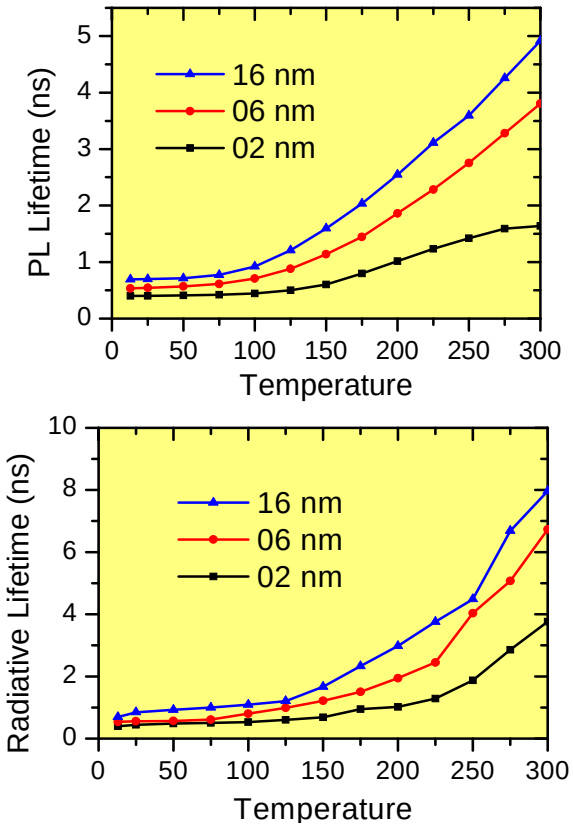

Fig. 4. Temperature dependence of PL and radiative lifetimes as a function of quantum well width.

temperature independent below 77K. This behavior indicates that the PL lifetime is dominated by the radiative lifetime up to room temperature, as poorer quality samples dominated by nonradiative effects exhibit an initial increase in PL lifetime with decreasing temperature due to the increase in nonradiative lifetime associated with the freezing out of nonradiative centers. Since the nonradiative lifetime is nearly infinite at our lowest measurement temperature of 13K, the PL lifetime at this temperature is approximately the radiative lifetime, with values of 400 ps, 540 ps, and 700 ps for the 2 nm, 6 nm, and 16 nm QWs, respectively, in agreement with theory. Moreover, the trend of smaller PL lifetime for narrower well width remains the same from low temperature to room temperature, resulting in room temperature radiative and nonradiative lifetimes of τ_{rad} = 3.75 ns and τ_{nr} = 2.9 ns for the 2 nm QW, τ_{rad} = 6.7 ns and τ_{nr} = 8.7 ns for the 6 nm QW, and τ_{rad} = 7.95 ns and τ_{nr} = 12.8 ns for the 16 nm QW. While both the low temperature and room temperature results confirm that the radiative lifetime is shorter for narrower well width, the extremely long nonradiative lifetimes indicate that defect-related nonradiative recombination is strongly suppressed for growth on bulk substrates, allowing the PL decay to

be dominated by the shorter radiative lifetime. These results lie in stark contrast to those on conventional nitride QWs on sapphire substrates, for which shorter nonradiative lifetimes associated with the high defect density and longer radiative lifetimes due to the field-induced decrease in wave function overlap lead to shorter PL lifetimes and weaker emission (Garrett et al., 2005). Thus, development of high quality nitride semiconductor heterostructures on bulk nonpolar substrates could be a potential breakthrough disruptive technology for development of visible and ultraviolet optoelectronic devices for Army applications.

3. THZ EMISSION FROM NONPOLAR NITRIDE SEMICONDUCTORS

Terahertz (THz) radiation from semiconductors illuminated by ultrafast optical pulses is commonly generated through in-plane carrier acceleration in electric fields created by externally biased photoconductive (PC) switches (Auston, 1975) or from a surge-current normal to the surface due to a built-in surface field or the photo-Dember field (Liu et al., 2006). Although the geometry of the biased PC antennas is more favorable for coupling out the THz radiation than that for other semiconductor-based THz sources employing transport normal to the surface (Shan et al., 2001), these PC switches require electrode processing and an external bias voltage, which is limited by the dielectric strength of air, to establish an in-plane electric field. Evidence of internal electric fields induced by stacking fault (SF)-terminated internal polarization in polar crystals such as ZnS, ZnTe, SiC and GaN has been observed (Neumark, 1962, Pal et al., 1991, Majewski and Vogl, 1998, Majewski et al., 2000, Juillaguet et al., 2007). In semipolar or nonpolar wurtzite crystals, for which there is a projection of the polar axis in the growth plane, the SF-induced electric fields associated with the termination of the internal polarization (Bernardini et al., 1997) along the polar <0001> direction at wurtzite domain boundaries also lie in-plane. The high fields within the wurtzite domains terminated by the SFs should point in the same direction, effectively creating an array of contactless PC switches that could significantly enhance THz emission from semiconductor surfaces under ultrashort pulse excitation.

The samples employed in this study were a ~1 μm-thick high SF-density (~ 1 X 10^6/cm) GaN epilayer grown by metalorganic chemical vapor deposition (MOCVD) on an m-plane 6H-SiC substrate with an AlN nucleation layer, and a ~330 μm-thick SF-free m-GaN substrate from Mitsubishi Chemical Co., Ltd. The samples are optically excited using ~150 fs pulses obtained from the third harmonic (266 nm) and second harmonic (400 nm) of a 250 kHz regenerative amplifier at 800 nm, as well as from the frequency doubled signal beam (350 nm) of an optical

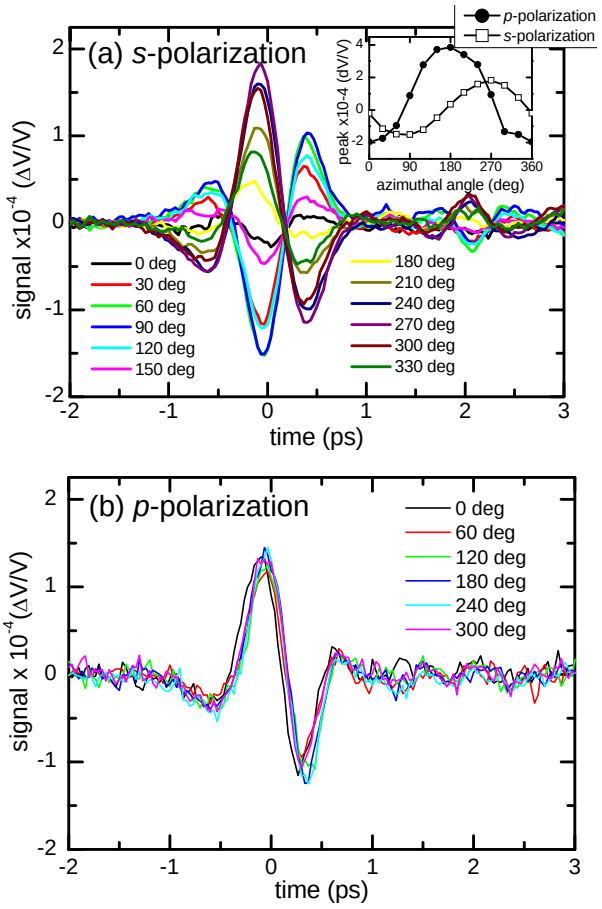

Fig. 5. (a) Dependence of *s*-polarized THz emission on sample angle for high SF *m*-GaN (top). Inset shows sample angle dependence of peak THz signals for both *s*- and *p*-polarization. (b) Sample angle independent *p*-polarized THz emission from SF-free *m*-GaN.

parametric amplifier pumped by the regenerative amplifier. The pump beam is incident on the GaN sample at 45° to the surface normal, and the subsequent THz emission is collected with a pair of parabolic mirrors for polarization sensitive ZnTe-based electro-optic sampling.

Figure 5 shows a comparison of the time domain THz emission for 266 nm fs pulse excitation of the high SF density m-GaN and the SF free m-GaN. The terms *p*- and *s*-polarization refer to the polarization parallel and perpendicular to the plane of incidence, respectively. At θ = 0°, the *c*-axis of the nonpolar sample is in the plane of incidence. For the high SF density sample, the measured *s*-polarized (*p*-polarized) THz waveform polarity flips as the sample rotates, reaching a peak positive signal at θ = 270° (180°) and a peak negative signal at θ = 90° (0°) when the *c*-axis is parallel or antiparallel to the *s*-polarization (*p*-polarization) detection direction, respectively (see inset). In contrast, the *p*-polarized THz waveform from the SF-free *m*-GaN has no dependence on

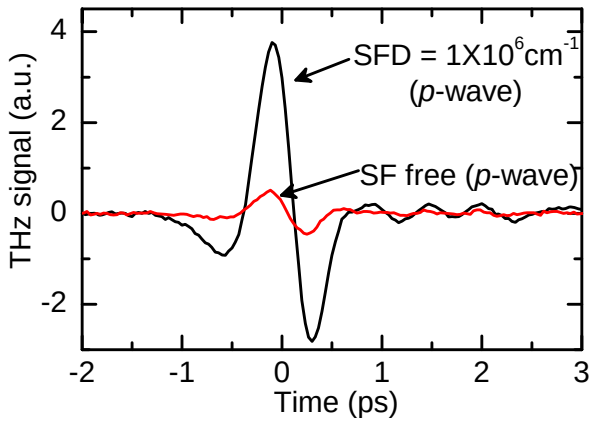

Fig. 6. Comparison of the THz signal from the high SF GaN sample and the SF-free GaN for 350 nm fs laser excitation.

sample rotation angle, and no *s*-wave component is observed from this sample.

The strong THz emission from the high SF density sample that exhibits a 360° periodicity with sample rotation and a polarity flip at 180° for polarization-sensitive detection is characteristic of real carrier transport in an in-plane electric field parallel to the c-axis. The observation that a similar phenomenon is not observed in the SF-free sample implies that this in-plane field is induced by zincblende stacking fault termination of the internal polarization at wurtzite domain boundaries (Fig. 2). At the wurtzite/zincblende interface, charge accumulation leading to strong electric fields parallel to the *c*-axis of the crystal occurs. In-plane transport of photoexcited carriers proceeds parallel to the electric field, leading to a THz radiation component polarized preferentially along this axis of the sample (Metcalfe et al., 2008). Rotating the *c*-axis by 180° also rotates the direction of the built-in field by 180°, causing the photoexcited carriers to accelerate in the opposite direction, with a reversal of the photoexcited carrier acceleration direction observed as a flip in the THz waveform polarity. The $\sin\theta$ dependence of and 90° shift between the *p*- and *s*-polarization curves (inset) indicates that the linearly polarized THz emission associated with in-plane carrier transport rotates with sample rotation. No optical rectification is observed; evidence of nonlinear polarization would appear as a $\sin(n\theta)$ (where $n>1$) dependence of the THz signal. Moreover, no dependence on pump polarization is found after accounting for absorption, and the THz signal vanishes for 400 nm excitation, indicating that the signal is associated with the generation and transport of real carriers.

The inset of Fig. 5 shows that the peak positive signal of the *p*-polarized THz signal is larger than the peak negative signal. This offset is due to the angle independent *p*-polarization signal, as observed in the SF-free sample and other semiconductors such as InN and InAs, which emanates from surface surge-currents and diffusion-driven carrier transport normal to the surface and is independent of the c-axis orientation (Chern et al., 2006). Although this signal is expected to be large due to the high excess electron energy (~1 eV) and small absorption depth (<50 nm) for 266 nm excitation, subtraction of the offset on the angular dependence of the peak *p*-polarized signal in the inset of Fig. 5 indicates that the component of the THz emission associated with the in-plane transport in the high SF-density sample is nearly 3 times greater. In a direct comparison between the SF-free sample and high SF sample, Fig. 6 shows that the THz signal from the high SF sample becomes ~7 larger than that from the SF-free sample for 350 nm excitation ,as the component of THz emission emanating from the in-plane transport remains robust, while the signal associated with the diffusion component of surface normal photocurrents becomes smaller, as expected for the lower excess electron energy (<100 meV) and increased absorption depth (~100 nm).

Majewski *et al*. (1998, 2000) have performed ab-initio calculations of zincblende inclusions embedded in bulk wurtzite GaN and concluded that charge buildup at the wurtzite/zincblende interfaces in GaN results primarily from the spontaneous polarization P_{sp} in wurtzite material, with a negligible contribution from the piezoelectric polarization. They also concluded that the interface charge can be calculated from the bulk spontaneous polarization. Using a thickness of the zincblende region (in this case, the I_1 type SF) of $d_{zb} \approx 3c_{wz}/2 = 8$ Å, where c_{wz} is the lattice constant of wurtzite GaN, a thickness of the wurtzite region of $d_{wz} \approx 1/n_{sf} = 100$ Å, where n_{sf} is the SF density, and $P_{sp} = -0.034$ C/m^2 (Ambacher et al., 2002), the maximum average in-plane electric field in the wurtzite region of an *m*-GaN sample with an I_1 type SF density of 1 X 10^6 cm^{-1} is estimated from Maxwell's equations with appropriate boundary conditions at the SF interface as ~290 kV/cm. This field is comparable to the bias fields applied to photoconductive (PC) switches using low-temperature grown GaAs (Tani et al., 1997), one of the best THz sources, but does not require electrode processing or an external bias, as the high SF density effectively creates an array of nanoscale contactless PC switches. This novel result may be exploited in InN and InGaN alloys with bandgaps more suitable for fs fiber laser excitation, potentially enabling improved efficiency of THz sources in compact, field-deployable THz spectroscopy systems.

4. CONCLUSION

Nonpolar nitride semiconductors are promising materials for next generation Army applications across

the electromagnetic spectrum. InGaN quantum wells on bulk stacking fault–free GaN substrates for visible emitters show enhanced radiative efficiency associated with reduced radiative lifetime and longer nonradiative lifetime, relative to conventional polar devices on sapphire substrates. In addition, even highly defective nonpolar nitride semiconductors with large stacking fault densities can be used as high efficiency THz sources, due to carrier transport in internal in-plane electric fields created by the termination of the in-plane polarization in wurtzite domains at zincblende SFs,. The estimated, maximum average in-plane electric field of ~ 290 kV/cm in the wurtzite regions for an I_1 type SF density of 1 X 10^6 cm^{-1} is comparable to the bias fields applied to PC switches using low-temperature grown GaAs, one of the best PC materials, but does not require electrode processing or an external bias. Comparison with THz emission from SF-free m-GaN indicates that the THz signal from SF-related in-plane carrier transport dominates that usually observed from carrier diffusion or surface surge-currents normal to the sample surface, even for high excess electron energies and short absorption lengths favorable to diffusive transport.

REFERENCES

Ambacher, O., J. Majewski, C. Miskys, A. Link, M. Hermann, M. Eickhoff, M. Stutzmann, F. Bernardini, V. Fiorentini, V. Tilak, B. Schaff, and L. F. Eastman, "Pyroelectric properties of Al(In)GaN\–GaN hetero- and quantum well structures", *J. Phys.: Condens. Matter*, Vol. 14, pp. 3399-3434, 2002.

Auston, D. H., "Picosecond optoelectronic switching and gating in silicon," *Appl. Phys. Lett.* Vol. 26, No. 3, pp. 101-103, 1975.

Bernardini, F., V. Fiorentini and D. Vanderbilt, "Spontaneous polarization and piezoelectric constants of III-V nitrides", *Phys. Rev. B*, Vol. 56, No. 16, pp. R10024-R10027, 1997.

Chern, G. D., E. D. Readinger, H. Shen, M. Wraback, C. S. Gallinat, G. Koblmüller, and J. S. Speck, "Excitation wavelength dependence of terahertz emission from InN and InAs", *Appl. Phys. Lett.* Vol. 89, Art. 141115, 2006.

Garrett, G.A., H. Shen, M. Wraback, B. Imer, B. Haskell, J. S. Speck, S. Keller, S. Nakamura, and S. P. DenBaars, "Intensity dependent time-resolved photoluminescence studies of GaN/AlGaN multiple quantum wells of varying well width on laterally overgrown a-plane and planar c-plane GaN", *Phys. Stat. Sol. (a)*, Vol. 202, pp. 846-849, 2005.

Grandjean, N., B. Damilano, S. Dalmasso, M. Leroux, M. Laügt, and J. Massies, "Built-in electric-field effects in wurtzite AlGaN/GaN quantum wells", *J. Appl. Phys.*, Vol. 86, No. 7, pp. 3714-3720, 1999.

Haskell, B. A., F. Wu, M. D. Craven, S. Matsuda, P. T. Fini, T. Fujii, K. Fujito, S. P. DenBaars, J. S. Speck, and S. Nakamura, "Defect reduction in (11$\bar{2}$0) a-plane gallium nitride via lateral epitaxial overgrowth by hydride vapor-phase epitaxy", *Appl. Phys. Lett.*, Vol. 83, No. 4, pp. 644-646, 2003.

Im, J. S., H. Kollmer, J. Off, A. Sohmer, F. Scholz, and A. Hangleiter, "Reduction of oscillator strength due to piezoelectric fields in $GaN/Al_xGa_{1-x}N$ quantum wells", *Phys. Rev. B*, Vol. 57, No. 16, pp. R9435-9438, 1998.

Iso, K., H. Yamada, H. Hirasawa, N. Fellows, M. Saito, K. Fujito, S. P. Denbaars, J. S. Speck, and S. Nakamura, "High Brightness Blue InGaN/GaN Light Emitting Diode on Nonpolar m-plane Bulk GaN Substrate," *Jpn. J. Appl. Phys.*, Vol. 46, pp. L960-L962, 2007.

Jho, Y. D., J. S. Yahng, E. Oh, and D. S. Kim, "Field-dependent carrier decay dynamics in strained $In_xGa_{1-x}N$/GaN quantum wells", *Phys. Rev. B*, Vol. 66, Art. 035334, 2002.

Juillaguet, S., J. Camassel, M. Albrecht, and T. Chassagne, "Screening the built-in electric field in 4H silicon carbide stacking faults," *Appl. Phys. Lett.*,Vol. 90, Art. 111902, 2007.

Liu, K., J. Xu, T. Yuan, and X-.C. Zhang, "Terahertz radiation from InAs induced by carrier diffusion and drift", *Phys. Rev. B*, Vol. 73, Art. 155330, 2006.

Majewski, J. A., G. Zandler, and P. Vogl, "Novel nitride devices based on polarization fields," *Phys. Stat. Sol. A*, Vol. 179, pp. 285-293, 2000.

Majewski, J. A., and P. Vogl, "Polarization and band offsets of stacking faults in AlN and GaN," *MRS Internet J. Nitride Semicond. Res.*, Vol. 3, Art. 21, 1998.

Neumark, G. F., "Theory of anomalous photovoltaic effect of ZnS," *Phys. Rev.*, Vol. 125, No. 3, pp. 838-845, 1962.

Pal, U., S. Saha, A. K. Chaudhuri, and H. D. Banerjee, "The anomalous photovoltaic effect in polycrystalline zinc telluride films," *J. Appl. Phys*,.Vol. 69, No. 9, pp. 6547-6555, 1991.

Shan, J., C. Weiss, R. Wallenstein, R. Beigang, T. F. Heinz, "Origin of magnetic field enhancement in the generation of terahertz radiation from semiconductor surfaces", *Opt. Lett.*, Vol. 26, No. 11, pp. 849-851, 2001.

Tani, M., S. Matsuura, K. Sakai, and S. Nakashima, "Emission characteristics of photoconductive antennas based on low-temperature-grown GaAs and semi-insulating GaAs", *Appl. Opt.*, Vol. 36, No. 30, pp. 7853-7859, 1997.

Waltereit, P., O. Brandt, A. Trampert, H. T. Grahn, J. Menniger, M. Ramsteiner, M. Reiche, and K. H. Ploog, "Nitride semiconductors free of electrostatic fields for efficient white light-emitting diodes", *Nature*, Vol. 406, pp. 865-868, 2000.

Wraback, M., G.A. Garrett, A.V. Sampath, and P.H. Shen, "Understanding ultraviolet emitter performance using intensity dependent time-resolved photoluminescence", *Int. J. High Speed Electron. and Systems*, Vol. 17, No. 1, pp. 179-188, 2007.